Michigan State University

National Superconducting Cyclotron Laboratory

SPECTROSCOPY OF THE ^{10}Li NUCLEUS

J.A. CAGGIANO, D. BAZIN, W. BENENSON, B. DAVIDS,
B.M. SHERRILL, M. STEINER, J. YURKON, A.F. ZELLER,
and B. BLANK

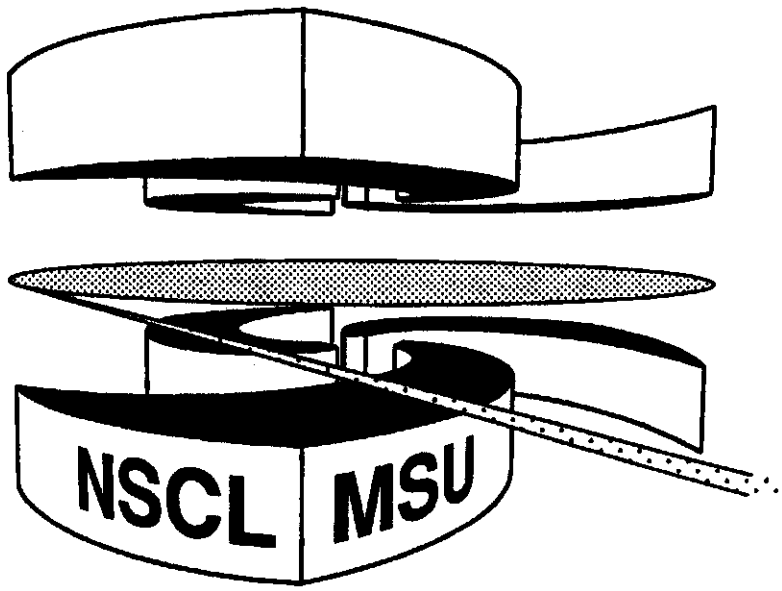

MSUCL-1103

JUNE 1998

Spectroscopy of the ^{10}Li nucleus

J.A. Caggiano, D. Bazin, W. Benenson, B. Davids, B.M. Sherrill, M. Steiner, J. Yurkon, A.F. Zeller

National Superconducting Cyclotron Laboratory, Michigan State University, *East* Lansing, MI *48824*

B. Blank

Centre d'Etudes Nucléaires de Bordeaux-Gradignan, F-331 75 GradignanCedex, France

(June 17, 1998)

Abstract

In an attempt to clarify the situation regarding the low-lying structure of ^{10}Li, we present a clean spectroscopic measurement of the structure of ^{10}Li with the ^{9}Be(^{9}Be,^{8}B)^{10}Li reaction at E(^{9}Be)=40.0(1) MeV/u using the newly commissioned S800 spectrograph at Michigan State University. A resonance is located at E_r = 0.265(20) MeV if the data near the ^{9}Li+n threshold is fit with a single p-wave resonance, while a better fit is achieved with s- and p-wave resonances at E_r = 0.030(25) and E_r = 0.310(20) MeV respectively. This is consistent with the supposition that there is a virtual s-wave state at threshold in ^{10}Li.

21.10.-k, 25.70.Hi, 27.20.+n

It is a well known effect of quantum mechanics that the wave function of a particle in a potential well can significantly penetrate the barrier if the separation energy is low. This effect is observed in nuclei when the last few valence nucleons are weakly bound. In some cases, such as ^{11}Li, the probability of finding a valence neutron outside the core nucleus is more than 90% [1]. Put another way, the valence rms radius for ^{11}Li is 9.5 fm while the ^{9}Li core rms radius is only 2.3 fm [2]. In this case the extent of the penetrating wave function is far longer than the range of the nuclear force. This type of nucleus is called a halo nucleus and represents a new form of nuclear matter, i.e. a central normal nucleus and a substantial halo of penetrating wave function. It is interesting to investigate how well standard nuclear models, such as the shell model, can describe the properties of these nuclei. Certain cases such as ^{11}Li are particularly interesting because here the last two neutrons are weakly bound. Hence the halo has two neutrons and the interactions of these neutrons in the diffuse nuclear surface largely determine the properties of ^{11}Li [3].

The nucleus ^{10}Li has been the subject of much experimental study, primarily in connection to its importance for the study of ^{11}Li. It has been speculated that the best model for ^{11}Li is a three-body system. Many authors have accurately calculated ^{11}Li properties with three-body models [4–6]. However, these attempts to understand ^{11}Li rely on the nature of the interaction between the two body subsystems, n-n and n-^{9}Li. The n-n interaction is well known, but the n-^{9}Li interaction is not well understood. All attempts to compare three-body and standard models of ^{11}Li rely on the ^{10}Li information, yet the existing experimental situation is unclear. In this letter we present the cleanest evidence to date on the low-lying structure of ^{10}Li of interest to three-body models of ^{11}Li.

It is most likely that the ground state of ^{10}Li is either a $0p_{1/2}$ or $1s_{1/2}$ neutron coupled to the $0p_{3/2}$ proton, giving rise to states with J^{π} assignments of $(1^+,2^+)$ or $(1^-,2^-)$, respectively. Theoretical arguments have been made as to why the ground state of ^{10}Li might be an s-wave state. Barker and Hickey predicted in 1977 that the ^{10}Li ground state is a non-normal parity virtual s-state [7], as is the case with ^{11}Be. Some shell model calculations [8,9] suggest that the s-wave (2^-) state is the ground state, while other calculations [10–12] suggest that

a p-wave state (1^+) may be the ground state.

There is no consensus on ^{10}Li structure based on experimental work [11,13–15] (Table I). Wilcox [13] saw roughly 30 counts with poor resolution in a peak identified as the ^{10}Li ground state unbound by 800 keV. Young [14] had roughly twice the number of events, and saw some evidence for a low-lying, possibly s-wave state at <100 keV in addition to a higher lying p-wave state at 540 keV. Amelin [16] observed a broad peak at 150 keV which was identified as the ^{10}Li ground state. Kryger [17] saw a narrow peak in a ^{9}Li-n relative velocity spectrum from the fragmentation of ^{18}O, which may be interpreted as a low-lying s-wave state at 50 keV or a higher lying state decaying to a ^{9}Li excited state. Bohlen [15] has seen several structures, in particular resonances at 240 and 530 keV, attributed to p-wave resonances. Unfortunately, most spectroscopic measurements of ^{10}Li structure to date have been plagued by poor statistics, poor resolution, target contaminants, or some combination of all three.

It is evident that the picture of ^{10}Li is cloudy at best. With this in mind, we set out to measure the low-lying resonance structure of ^{10}Li using the newly-commissioned S800 spectrograph at Michigan State University [18]. Our goal was to perform a clean, high-resolution, high-statistics spectroscopic measurement of ^{10}Li near threshold.

The spectrometer is designed to have an energy resolution of $E/\Delta E = 10{,}000$, an angular resolution of 2 milliradians, and a 20 msr solid angle acceptance. It consists of a beam analysis line and the spectrograph proper. The beam analysis line is very similar to the A1200 fragment separator at MSU [19], but with larger acceptance and better resolution. The spectrograph proper consists of a large, superconducting quadrupole doublet followed by two 75-ton superconducting dipole magnets. The detectors in the focal plane consist of two position tracking detectors separated by approximately one meter, an ion chamber for energy loss measurements, and three thick plastic scintillators for total energy measurement (Fig. 1).

The spectrometer was operated in dispersion-matched, energy-loss mode to cancel the 0.08(1)% intrinsic beam energy spread. Ray-tracing techniques were used to reconstruct the

energy of the ejectile from the target. This is done by using the measured magnetic field data as input to the particle optics code COSY [20]. COSY calculates a transfer matrix from the target to the focal plane. Then, by assuming the beam spot is small and the dispersion matching is perfect, the transfer matrix is inverted. By measuring horizontal and vertical positions and angles in the focal plane, it is possible to deduce the energies, angles, and vertical position of the emerging nuclei from the reaction in the target using the procedure described in [21].

We chose the ^{9}Be(^{9}Be,^{8}B)^{10}Li reaction because it is reported to have a reasonably large cross section [13]. Also, the ^{8}B ejectile has a much different rigidity than other competing reactions providing a relatively contaminant-free focal plane. A beam of 40.0(1) MeV/u ^{9}Be was used to bombard three targets: 1.22(5) mg/cm^2 Be, 0.80(5) mg/cm^2 carbon, and a 0.45(3) mg/cm^2 Be target on a formvar backing. The ^{8}B reaction products were swept and focussed onto the focal plane of the spectrograph, where the two transverse positions and angles, and total energies of the ^{8}B ions were measured. The reaction scattering angles and energies were reconstructed with ray-reconstruction techniques [21] as described above. We used the ^{12}C(^{9}Be,^{8}B)^{13}B reaction as an energy calibration (ground state Q-value = -28.1356 MeV [22]). This reaction populated several known states in the ^{13}B nucleus which surround the location of the lowest observed ^{10}Li peak, illustrated in Fig. 2.

Elastic and inelastic scattering of the incident ^{9}Be beam off the targets provided calibration of the scattering angle and spectrograph bending radius. The small amount of hydrogen and oxygen contaminants in the carbon target as well as the formvar backing (carbon, hydrogen, and oxygen) on the thin beryllium target provide excellent scattering angle calibration ($\pm 0.05°$). The relationship between the bending radius of the spectrograph and the focal plane position was calibrated by sweeping the elastically-scattered peak across the focal plane by varying the magnetic field. The known bend radius of the S800 was used to determine the beam energy of 40.0(1) MeV/u.

Figure 2 shows energy spectra of the ^{8}B particles following the ^{12}C(^{9}Be,^{8}B)^{13}B and ^{9}Be(^{9}Be,^{8}B)^{10}Li reactions at 40.0(1) MeV/u. The scattering angle acceptance for the spectra

was 3.5-8.3 degrees in the lab. The spectra are summed over all angles with the energy for each angle shifted to what it would be at 0°. Known states in ^{13}B at 3.6810(45) MeV and 6.425(7) MeV were used for energy calibration.

The expected line shapes of the states in ^{10}Li have been calculated before by Young et al. [14] and Bertsch et al. [6]. The shapes for the p-wave states are well parameterized by a Breit-Wigner shape (with resonance energy E_r and width Γ) multiplied by an $E^{3/2}$ term. The calculations of [14] were fit with this parameterization and one from [6], the former fitting the calculations slightly better, so we used this one. Both parameterizations fit our data equally well. The parameterization of the s-wave state was adopted from Bertsch, et al. [6], and contains two parameters; a, the scattering length and α, the decay constant in the asymptotic radial wavefunction, $\psi(r) \propto e^{-\alpha r}/r$ [6]. The scattering length a is related to α, and the value of a was constrained to be $a = -1/(1.7\alpha)$, consistent with [6]. The angular momentum barrier of the p-wave states causes their width to increase more slowly with resonance energy than the s-wave states. For example, a 250 keV p-wave state is estimated to have a width around 100 keV, while an s-wave state at the same location has a width well over 1 MeV.

The ^{10}Li spectrum (Fig. 3) was fit using a convolution of the calculated line-shape with the experimental resolution. The function minimization routine AMOEBA was adopted from Press et al. [23], and used to perform χ^2 minimization. The spectrum was first fit from -0.5 to 7.5 MeV relative energy to determine the parameters of the higher lying peaks in the spectrum. Then, the lowest lying peak was fit with p-wave or s-wave and p-wave parameterizations while constraining the higher lying states to their previously fit values. The fit corresponding to the extracted states is shown in the top panel of Fig. 3.

An acceptable overall fit is achieved with only a p-wave state close to threshold, or a combination of s-wave and p-wave states close to threshold (Fig. 3). The lowest lying structure fit with only a p-wave has a peak at 270(30) keV, while the s-wave and p-wave fit has the p-wave at 320(30) keV, with the s-wave state peaking at 30(30) keV. The width of the p-wave state for both fits is 80(50) keV. The other structures were fit with the p-wave

parameterization (s-wave states would be too broad this high above the threshold). The combination provides a substantial reduction in the reduced χ^2 in the region -0.5 to 1.0 MeV, from 3.3 to 1.6, consistent with the observation of a low-lying s-wave state.

The thinner target data set has better resolution but is contaminated by reactions with carbon and oxygen in the formvar backing, and has one-third the counts of the thicker target data set. We scaled, moved, and adjusted the width of the fit spectrum from the carbon target then subtracted it from the thin target spectrum. The lowest lying structure fit with only a p-wave has a peak at 240(30) keV, while the s-wave and p-wave fit has the p-wave at 270(30) keV, with the s-wave state peaking at 40(40) keV. The width of the p-wave state for both fits is slightly narrower than for the thicker target at 70(50) keV. An average of the two measurements, weighted by the number of counts in the lowest peak, gives E_r=265(20) for the p only fit, and E_r=30(25) (with a scattering length of -10(5) fm) and E_r=310(20) for the s and p fit, respectively. All peak parameters are summarized in Table II.

The errors were determined using a quadrature sum of several sources. Target thickness, beam energy, spectrometer angle, and ray-tracing techniques all play small roles (<10 keV) because the calibration and the measurement used the same reaction, (^{9}Be,^{8}B). The uncertainties on the mass (1 keV) and excited states ($\leq$7 keV) in ^{13}B are included. Statistical errors on the parameters vary from 1-10%, and dominate the uncertainty in most parameters.

Because the lowest strong peak is relatively narrow, we conclude that it must be dominantly a p-wave state, based on previous calculations [6,14]. However, one reference suggests that the spin-parity assignment of the state can not be extracted by line-shape alone [24]. Clearly a measurement sensitive to the quantum numbers of the states should be performed.

These measurements represent vast improvement on a cloudy picture of ^{10}Li. Taken with results from Kryger, Young, Bohlen, and Zinser (analyzed by Bertsch et al.) they provide evidence for the existence of two low-lying p states, one at 250-300 keV, and another at 500-550 keV, and a very low-lying s-wave state. The quantum numbers and exact line shapes of the states remain undetermined. It is interesting that the values of the present experiment

match quite well the extracted "best fit" analysis of Bertsch et al. [6] (Table I). Of further interest is the finding by Thompson and Zhukov that the combined existence of a low-lying s state and a p state in the range of 200-300 keV in ^{10}Li is required to reproduce the ^{11}Li binding energy in a three body model [4].

In summary, we have used the ^{9}Be(^{9}Be,^{8}B)^{10}Li reaction to make a clean spectroscopic measurement of ^{10}Li structure. Asymmetric s-wave and p-wave line shapes were used to fit the data, and the results are summarized in Table II. The s- and p-wave fit to the lowest lying portion of the spectrum yields the best fit, with the s-wave (at 30(25) keV, scattering length of -10(5) fm) integral strength being 25(10)% that of the p-wave at 310(20) keV. A slightly worse but acceptable fit with only a p-wave resonance was made with the resonance at 265(20) keV. A different reaction or the same reaction made at zero degrees may populate the s-wave state more. In particular, it would be desirable to repeat the Young [14] experiment with better resolution.

This work was supported by the U.S. National Science Foundation, grant number PHY-9528844.

REFERENCES

[1] K. Riisager, Rev. Mod. Phys. 66, 1105 (1994).

[2] J.S. Al-Khalili and J.A. Tostevin, Phys. Rev. Lett. 76, 3903 (1996).

[3] P.G. Hansen et al., Ann. Rev. Nuc. Part. Sci. 45, 591 (1995).

[4] I. Thompson and M. Zhukov, Phys. Rev. C49, 1904 (1994).

[5] H. Esbensen, Phys. Rev. C56, 3054 (1997).

[6] G.F. Bertsch et al., Phys Rev C57, 1366 (1998).

[7] F.C. Barker and G.T. Hickey, J. Phys. G3, L23 (1977).

[8] B.A. Brown, Proc. Int. Conf. Exotic Nuclei and Atomic Masses, Arles France, 451 (1995).

[9] N.A.F.M. Poppelier et al., Z. Phys. A346, 11 (1993).

[10] J. Wurzer and H.M. Hofmann, Z. Phys. A354, 135 (1996).

[11] H.G. Bohlen et al., Z. Phys. A344, 381 (1993).

[12] P. Descouvemont, Nuclear Physics A626, 647 (1997).

[13] K.H. Wilcox et al., Physics Letters 59B, 142 (1975).

[14] B.M. Young et al., Phys Rev C49, 279 (1994).

[15] H.G. Bohlen et al., Nuclear Physics A616, 254c (1997).

[16] A.I. Amelin et al., Sov. J. Nucl. Phys. 52, 782 (1990).

[17] R.A. Kryger et al., Phys. Rev. C47, R2439 (1993).

[18] J.A. Nolen Jr., et al., MSU-NSCL report No. MSU-694, (1989).

[19] B.M. Sherrill, et al., Nucl. Instrum. Methods B70, 298 (1992).

[20] M. Berz et al., Nucl. Instrum. Methods A 298, 473 (1992).

[21] M. Berz et al., Physical Review C47, 537 (1993).

[22] G. Audi and A.H. Wapstra, Nuclear Physics A565, 1 (1993).

[23] W.H. Press et al., Numerical Recipes in C (1992).

[24] K.W. McVoy and P. Von Isacker, Nuc. Phys. A576, 157 (1994).

[25] M. Zinser et al., Nuclear Physics A619, 151 (1997).

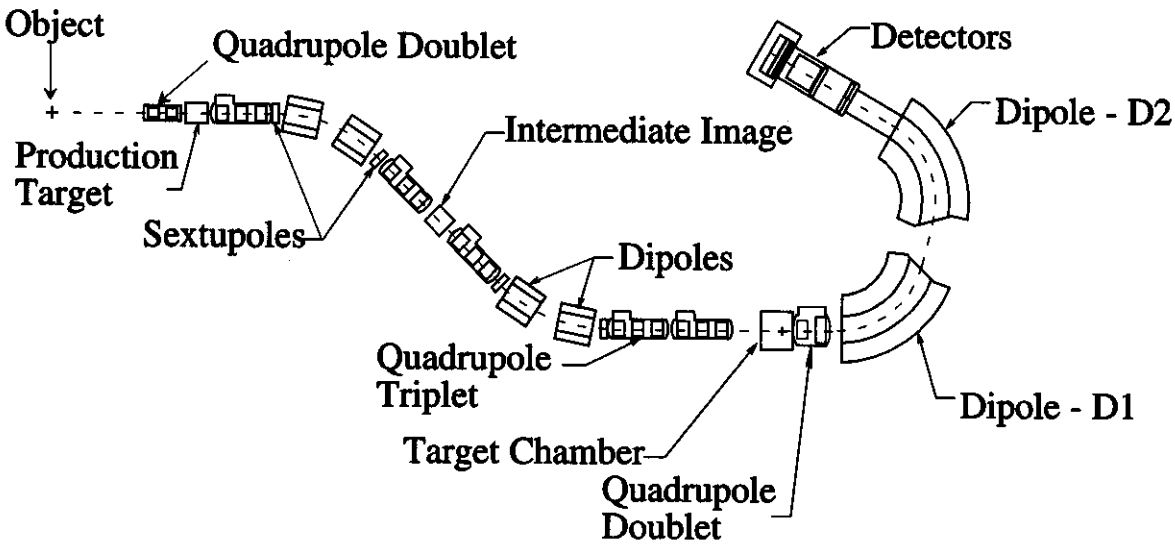

FIG. 1. Schematic layout of S800 spectrometer at MSU.

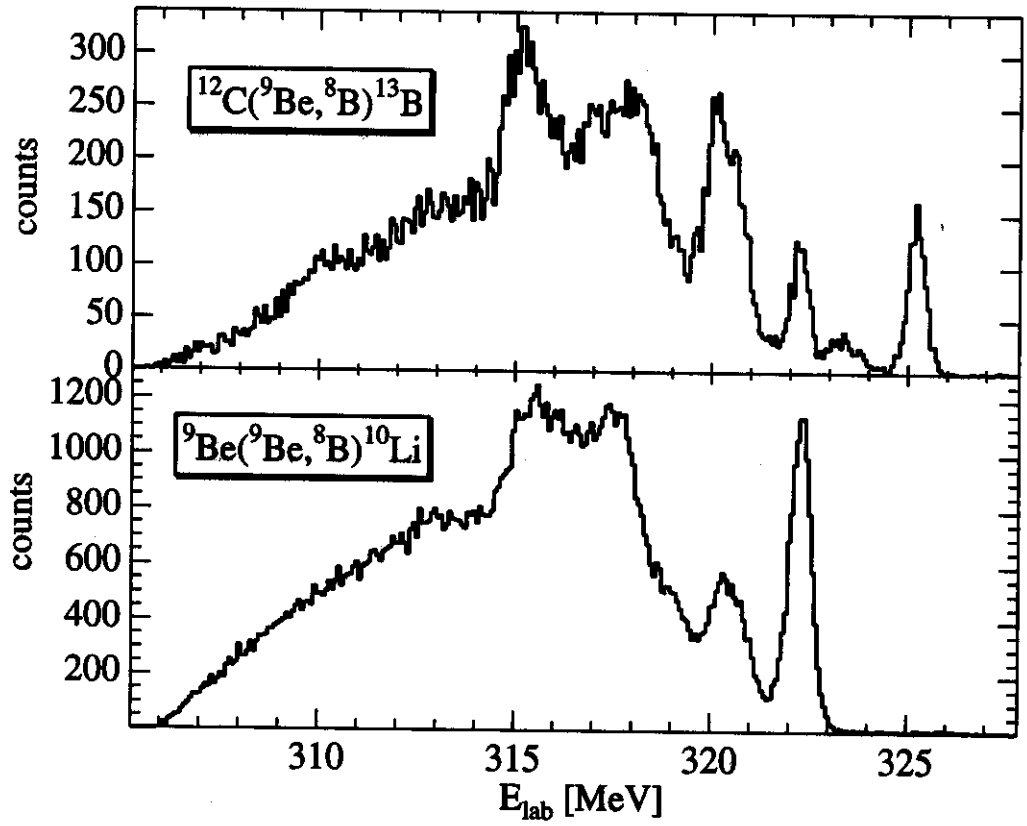

FIG. 2. ^{8}B energy spectra for the two reactions. See text for details.

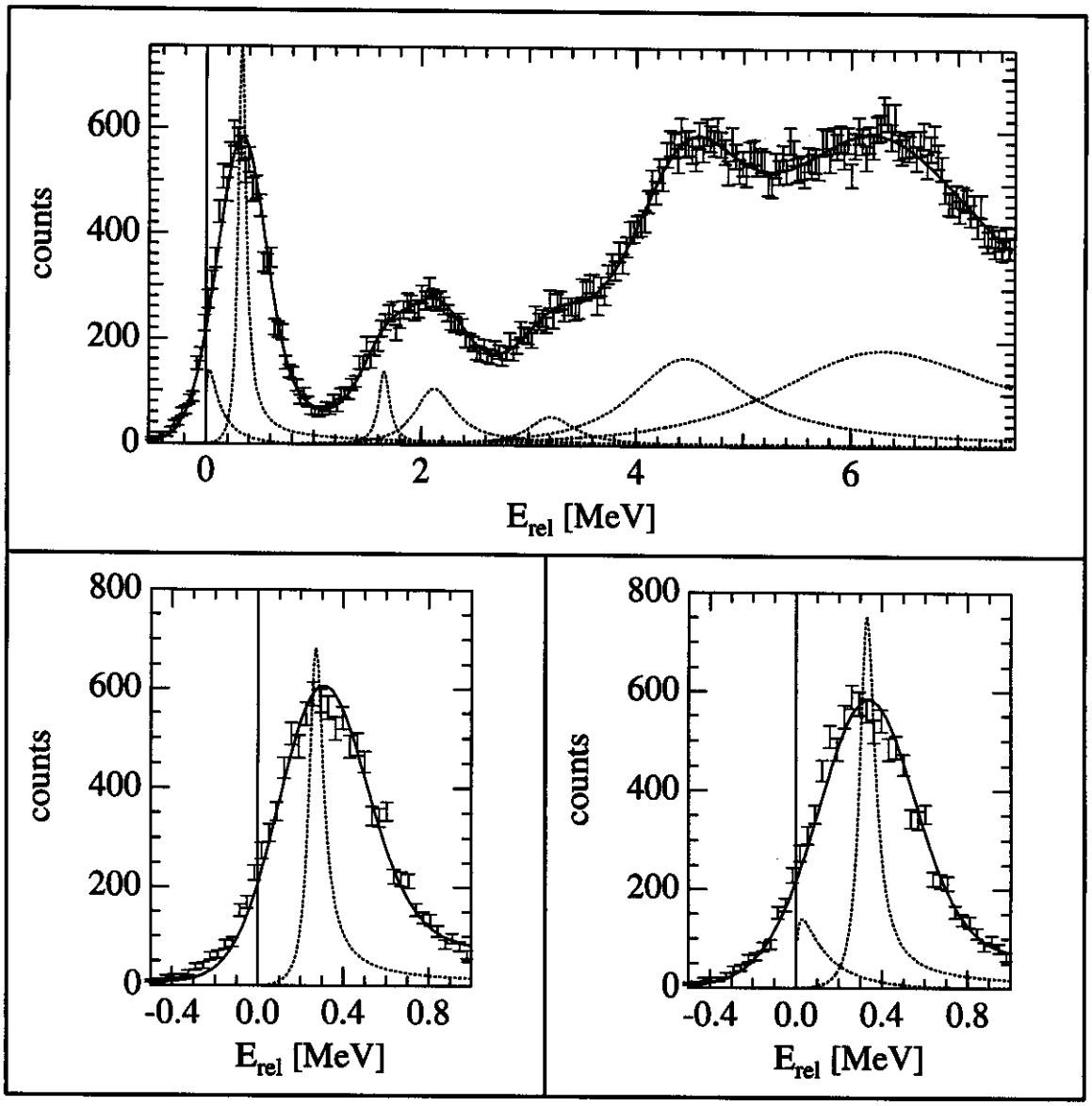

FIG. 3. ^{10}Li relative energy spectrum for the reaction ^{9}Be(^{9}Be,^{8}B)^{10}Li. The top panel shows parameterized line shapes fit to the data. The dashed lines are the individual resonance shapes and solid line through the data represents the fit of those resonances folded with the experimental resolution. The lower left panel is an enlargement of the region close to threshold with only a p-wave fit. The lower right panel shows the same energy region, but with an s-wave and p-wave fit to the data.

TABLES

TABLE I. Previous measurements of ^{10}Li low-lying resonances. The energies, widths, and uncertainties of the observed resonances below -S_n=1 MeV are listed as well as the year that the data were published, and any assignment given by the authors.

Author	Year	Reaction	-S_n[MeV]	Γ[MeV]	Assignment
Wilcox et al. [13]	1975	^{9}Be(^{9}Be,^{8}B)^{10}Li	0.80(25)	1.2(3)	g.s.
Amelin et al. [16]	1990	^{11}B(π^-,p)^{10}Li	0.15(15)	<0.4	$s_{1/2}$ g.s.
Kryger et al. [17]	1993	^{18}O fragmentation	<0.15		g.s.
			or ≈ 2.5		excited state
Young et al. [14]	1994	^{11}B(^{7}Li,^{8}B)^{10}Li	0.54(6)	0.36(2)	$p_{1/2}$
			<0.10	<0.23	$s_{1/2}$ g.s.
Bohlen et al. [15]	1997	^{9}Be(^{13}C,^{12}N)^{10}Li	0.53(6)	0.30(8)	
		^{10}Be(^{12}C,^{12}N)^{10}Li	0.24(6)		$p_{1/2}$
Zinser et al. [25]	1997	^{11}Li breakup	0.21(5)	0.12(+0.10,-0.05)	
			0.62(10)	0.6(1)	
Bertsch et al. [6]	1998	^{11}Li breakup[a]	a = -1.75(75) fm		$s_{1/2}$ g.s.
			0.30(5)		$p_{1/2}$

[a]This is a reanalysis of Zinser data [25].

TABLE II. Peaks observed in ^{10}Li from the ^{9}Be(^{9}Be,^{8}B)^{10}Li reaction in the present work. The results from only p-wave fit (6 peaks) are given on the left, and from s-wave and p-wave fit (7 peaks) are given on the right. The parameters for the s-wave state are α and the scattering length, a.

p-wave states only		s- and p-wave states	
peak location [MeV]	width [MeV]	peak location [MeV]	width [MeV]
		(α =) 13(7) MeV/c	(a =) -10(5)fm
0.265(20)	0.08(5)	0.310(20)	0.08(5)
1.63(17)	0.13(5)	1.63(17)	0.13(5)
2.08(12)	0.43(10)	2.08(12)	0.43(10)
3.17(27)	0.54(20)	3.17(27)	0.54(20)
4.44(14)	1.29(10)	4.44(14)	1.29(10)
6.09(19)	2.62(20)	6.09(19)	2.62(20)